SW and S-N trending fractures of the Yuntdağ volcanic III the NE-SW trending fractures are predominant in the south-west area of Çam Tepe, whereas in the eastern area, NW-SE fractures are abundant.

It is considered that the fractures are accompanied by the activity of a NW-SE trending graben near Çam Tepe and the NE-SW fault running through the west side of Çam Tepe.

2. Around Payam Tepe

Fractures are observed mainly in the Yuntdağ valcanics III in this area.

As a whole, fractures trending NW-SE are recognised. In these fractures, there are 2 groups trending NWN-SES and WNW-ESE direction. Many fractures are accompanied by hydrothermal veins.

3. Around Dede Tepe

In this area, the fractures are measured in the Yuntdağ volcanics I, the Demirtas pyroclastic rocks and the Yuntdağ volcanics III.

The NW-SE trending fractures are dominant in the Yuntdağ volcanics III, whereas in the Yuntdağ volcanics I and the Demirtas pyroclasitic rocks, there fractures of NE-SW and E-W direction. The fractures appear to be affected by the activity of the NW-SE fault running through the northern side of Dede Tepe and the WNW-ESE trending graben.

4. Around Maşat Tepe and Kargın Tepe

In this area, the NW-SE trending fractures clearly predominate. A few NE-SW direction fractures in the Yuntdağ volcanics I are found to the west of Maşat Tepe.

It seems that the fractures accompany the NW-SE fault forming the graben.

5. Around Ballıca Tepe

In this area, NW-SE trending fractures in the Yuntdağ volcanics III are few and E-W or WNW-ESE faults are abundant.

These fracture trends are different from those of the other area. That is, to the east of Kaynarca the fractures seem to be influenced by the movement of a WNW-ESE graben.

(b) Hydrothermal veins

Hydrothermal veins are largely found around Bayram Tepe and Eşkinburnu Tepe as shown in Fig. II.3.9.

At Bayram Tepe, 2 km east of Kaynarca, there are so many NW-SE trending veins in the Yuntdağ volcanics I as if they are sinter. The veins contain idiomorphic crystals of calcite and aquartz. Based on the results of homoginization temperature measurements in calcite, the homoginization temperature indicates 120°C to 150°C. This means that calcite was formed at about 50 m depth. This area was probably later uplifted and eroded, resulting in surface outcrop.

On the otherhand, the large silica veins which strike N30° to 35°W, dip 70° to 90°, range in width 10 to 100 cm are found in northeast area of Eşkinburnu Tepe. Some veins are well-exposed and extend about 100 m along the strike. Moreover, on the south side of Dede Tepe and Eşkinburnu Tepe, silica veins often form along NW-SE trending fractures. These veins develop in the Dikili lava and they appear to be formed by recent geothermal activity.

As shown in Fig. II.3.10, there are many NW-SE trending hydrothermal veins. Large veins are concentrated in the same direction. From the fact, the NW-SE trending fractures seem to be related to the geothermal activity in the area.

(c) Conclusion of fracture pattern and stress field

The fracture pattern for each formation in the survey area is given in Fig. II.3.11.

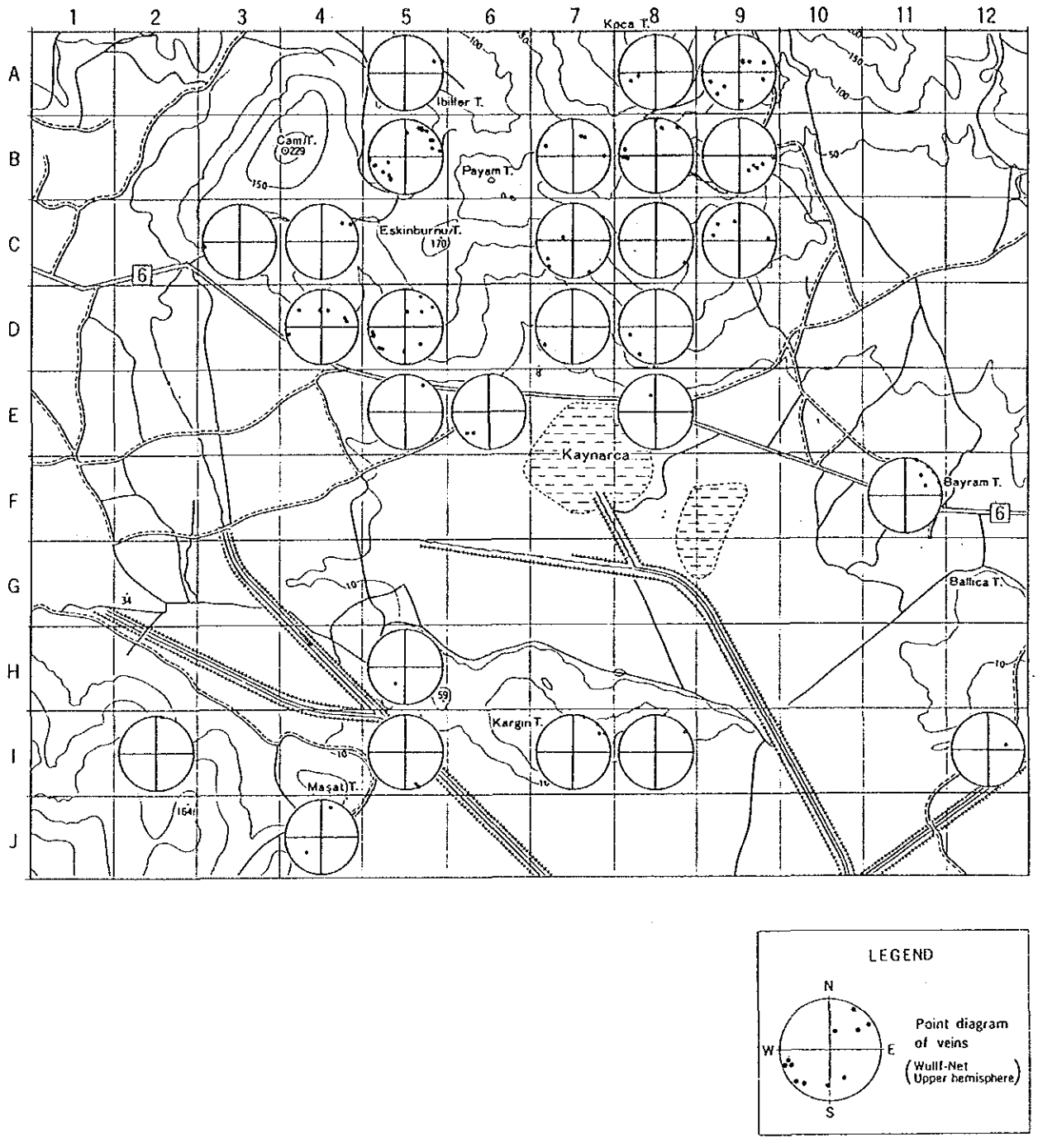

Fig. II.3.9 Pattern of hydrothermal veins in the Kaynarca geothermal area

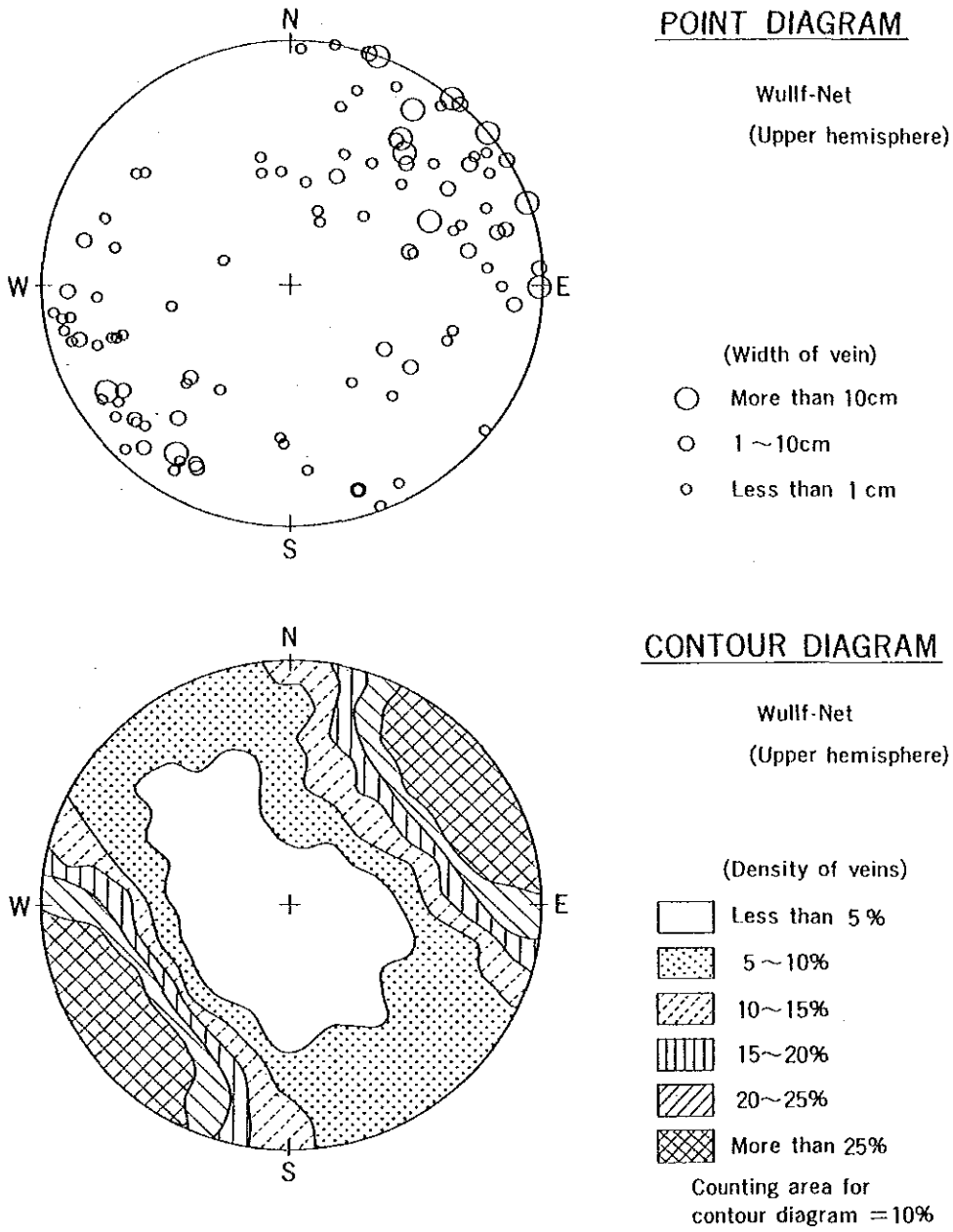

Fig. II.3.10 Plot of width and orientation of hydrothermal veins in the Kaynarca geothermal area.

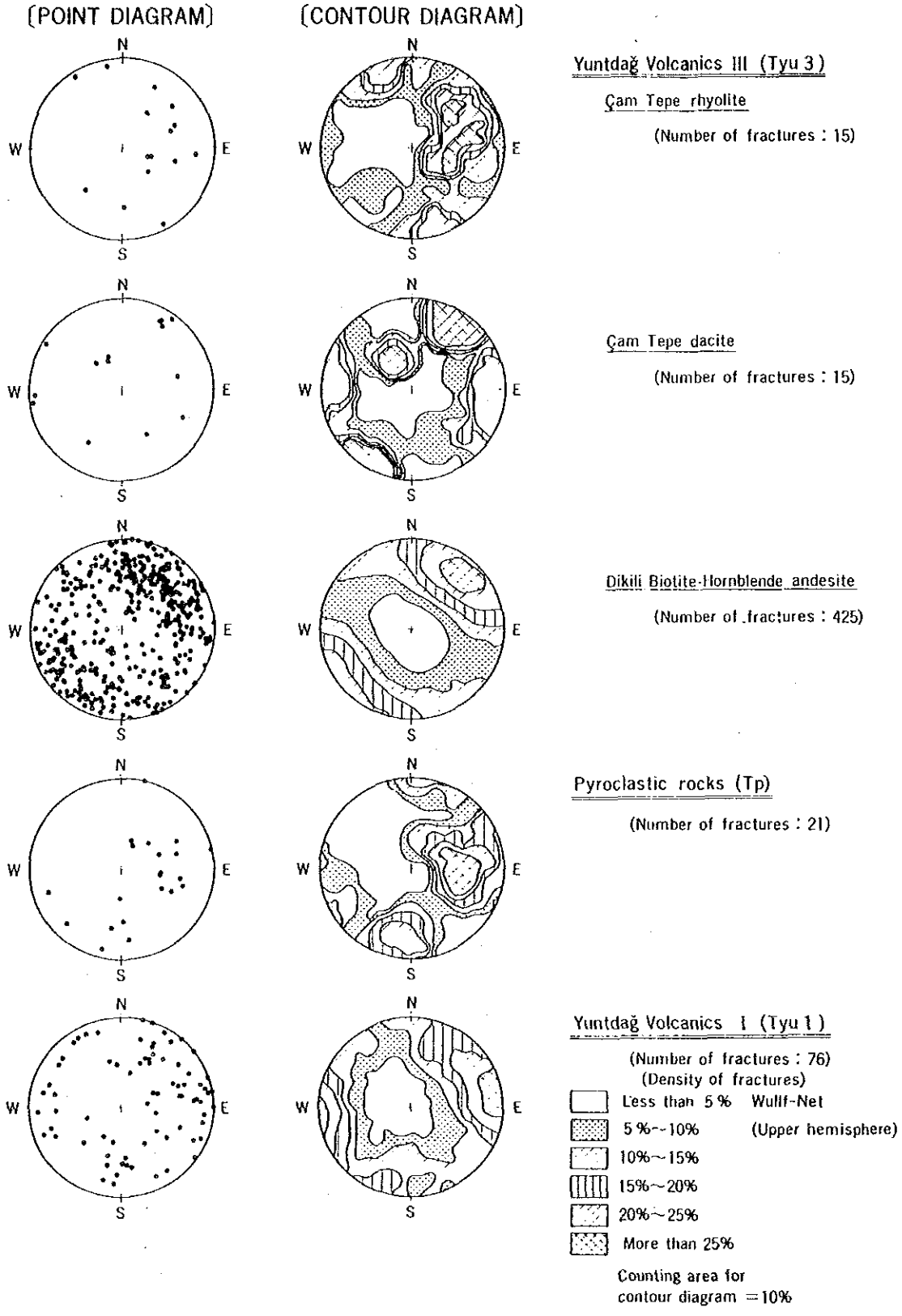

Fig. II.3.11 Fracture pattern in each formation

In the Yuntdag volcanics I which is the oldest formation in the survey area, the direction of fractures scattered and there is no dominant direction. It shows the Yuntdağ volcanics I have been influenced by many different tectonic movements.

The activity of the NW-SE trending faults began after the eruption of the Yuntdağ volcanics I. This activity formed the NW–SE to WNW-ESE graben which is controlled by NW-SE trending step faults falling toward the lowland in the center of the survey area. Most of these tectonics were completed before the Yuntdag volcanism III erupted. However, the activity of NW-SE trending faults had continued during Yuntdağ volcanism III. Then, may NW-SE trending fractures and hydrothermal veins were formed in Yuntdağ volcanics III as shown in Fig. II.3.11.

After that, the NW-SE trending faults appear to have been formed at the same time as the Çam Tepe dacite and rhyolite eruption. N-S and NW-SE trending fractures are found in the Çam Tepe dacite, rhyolite and the Demirtas pyroclastic rock around Çam Tepe.

Fig. II.3.12 shows the results of the stress field analysis using the fractures of the Yuntdağ volcanic III. When the stress field is presumed, a pair of conjugate fractures is usually used. When the conjugate fractures are decided, the following conditions are necessary.

a. The characters of fractures are similar

b. The fractures cut each other and are formed at same time

c. The direction of movement (sense) of fractures is contrary to each other.

In this survey, the pair of conjugate fractures could not be decided in the field because most outcrops in the survey area were made up of volcanic rocks. Also road cuttings which give fresh sections of the geological formation are few. The left side of Fig. II.3.12 shows the point diagram and contour diagram of fractures in the Yuntdağ volcanics III. As mentioned above, conjugate fractures were not decided then three groups A-A',

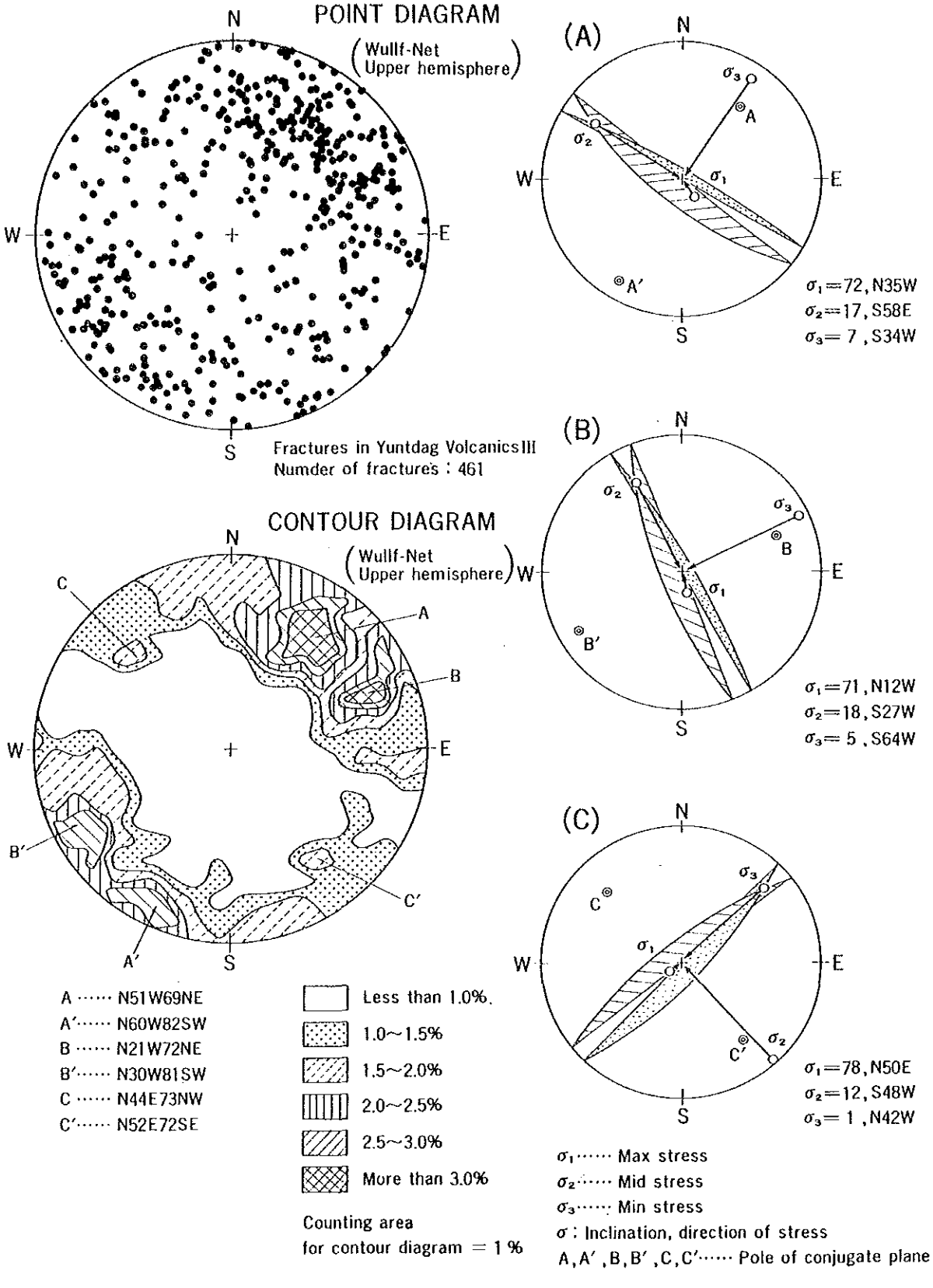

Fig. II.3.12 Presumed stress field in the Kaynarca geothermal area

B-B', C-C' which are found as a pair in many parts of the survey area were determined. A-A' group and B-B' group indicate fractures of NW-SE direction and C-C' group indicate fractures of NE-SW direction. Assuming that they are conjugate fractures, the analysis of the stress field was carried out. The results are shown in the right side of Fig. II.3.12.

The presumed stress field of (A) and (B) in Fig. II.3.12 indicates that NW-SE trending fractures of A-A' and B-B' were formed in the tension field of NE-SW. As already stated by DUMONT et.al. (1979), J. ANGELIER et.al. (1980), in the western Anatolia, NW-SE to E-W trending grabens are formed in the NNE-SSW to NE-SW trending tension field which continued from the late Miocene until the present time in spite of a few interruptions. The results of the stress field analysis shown in Fig. II.3.12 (A), (B), coincide with the above theory.

Meanwhile, Fig. II.3.12 (C) shows that fractures of C-C' are formed in the NW-SE trending tension field. These fractures are found around Çam Tepe. Before the Çam Tepe lava erupted, the NW-SE trending fault began to move in the NW-SE trending tension field. However, it is thought that the influence of this fault activity is not so great in the survey area because NE-SW trending fractures are comparatively few.

(4) Geothermal activity

The first geothermal activity in the survey area appears to have existed around Kocaoba and Dikili Ilıcasi. The activity is derived from the post volcanic action of the Yuntdağ volcanism I during Miocene time. A silicified zone was formed by the geothermal activity along NW-SE trending faults around both Kacaoba and Dikili Ilıcasi.

After the Yuntdağ volcanics I erupted, large scale tectonic movements resulted in the NW-SE trending graben in the center of the survey area. The geothermal activity accompanied by Demirtas felsic volcanism and Yuntdağ volcanism II is not found in the survey area.

After that, Yuntdağ volcanism III erupted large volume of lava. In the Dikili Lava of the Yuntdağ volcanics III, many fractures and hydrothermal veins are found. From this fact, it is inferred that the activity

of NW-SE trending faults continued after Yuntdağ volcanism III, so that the geothermal system is still active. When the Çam Tepe dacite and rhyolite erupted, the NE-SW trending faults were formed. The geothermal activity of the time appeared to be small scale because there are few NE-SW trending hydrothermal veins.

Hardly any hydrothermal altered zones are found in the Sulu Kaya lava and Koca Tepe lava which represent the latest period of volcanism of the Yuntdağ volcanism III. However, the two volcanoes are located between Kocaoba hot spring, and Kaynarca hot spring. Therefore, the heat source for the present geothermal activity is presumed to be related to the post volcanic action of these volcanic events.

Based on this survey, the geothermal structure of Kaynarca area was drawn as shown in Fig. II.3.13.

The subsurface structure around Kaynarca hot spring is characterized by NW-SE trending step faults. As shown in Fig. II.3.13, pre-Tertiary basement forms the NW-SE trending horst in the southern area of Dikili Ilıcasi, around Sulukaya and Koca Tepe and the NW-SE or WNW-ESE trending graben between Dikili Ilıcasi and Kaynarca.

Tectonic movement appears to continue from the end of the Yuntdağ volcanism I to Yuntdağ volcanism III. In the depression zone, the Soma formation, Demirtas pyroclastic rocks and Yuntdağ volcanics III were deposited thickly.

The recharging area of the Kaynarca hot water is assumed to be located in the northeastern part of Kaynarca and the western foot of Kozak massiff. The water recharged at a deep level is heated mainly by conductive heat from magmatic emission.

In the Kaynarca geothermal area, the reservoir is expected to exist at the boundary of the basement rocks and Yuntdağ volcanics I, in the fracture zones around faults and in the fractured zones in the Yuntdağ volcanics I at great depth. At the same time, argilization of the interbedded tuff breccia in the Yuntdağ volcanics I formed an impermeable zone resulting from self sealing by hot water comming up. Accordingly, it is thought that the formations form a cap rock which separates shallow cool water from the deep geothermal reservoir. Some hot water comes up along faults from these reservoirs and are observed

JAPAN INTERNATIONAL COOPERATION AGENCY — GENERAL DIRECTORATE OF MINERAL RESEARCH AND EXPLORATION

GEOTHERMAL DEVELOPMENT PROJECT
IN
DIKILI-BERGAMA FIELD

Fig. Ⅱ. 3.13

Geothermal structure of the Kaynarca geothermal area

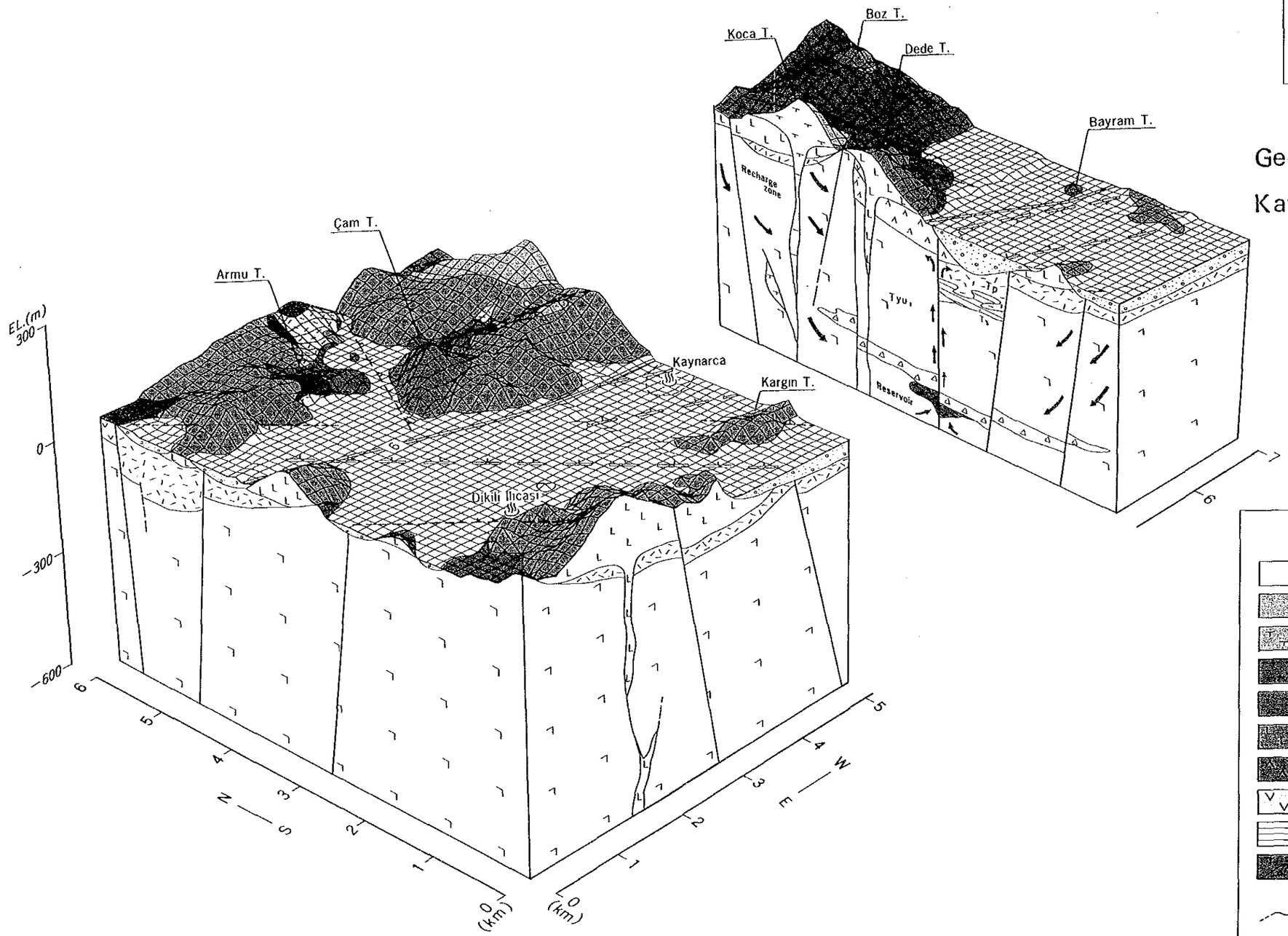

LEGEND

- Alluvium
- Yuntdağ Volcanics III
  - Sulu Kaya biotite-hornblende andesite
  - Koca Tepe biotite-hornblende andesite
  - Çam Tepe rhyolite
  - Cam Tepe biotite dacite
  - Dikili biotite-hornblende andesite
  - Koca Ağil horndende andesite
- İslamlar pyroxene andesite (Yuntdağ volcanics II)
- Ts : Soma Formation
- Tyu 1 : Yuntdag Volcanics I
- Fault
- Altered zone
- Upflow of thermal fluid
- $HCO_3(-SO_4)$ type reservoir
- Inflow of cold water
- Hot spring

at the surface as a hot spring and fumarole around Kaynarca. In addition, the promissing area of geothermal activity extends from WNW-ESE to NW-SE trending as a center of Kaynarca judging from the geological structure and the fracture pattern analysis.

II.3.2 CSAMT survey

1. Objectives

The CSAMT survey was carried out in order to understand the geoelectrical structure of the most prospective area, and then to select the site for the heat flow measuring hole.

2. Survey procedure

(1) Measuring procedure

Fig. II.3.14 shows the survey configuration for the CSAMT measurement. As shown in the figure, the measurement was carried out by two parties the receiver party and the transmitter party. The transmitter party sent electromagnetic signals through the current dipole which was arranged in a straight line on the ground for 4 km, and the currents ranged from 1 to 4 amperes, and the frequencies ranged from 0.167 to 512 Hz. The receiver party measured the electromagnetic signals using maximum eight non-polarizable electrodes and a coil which were set very far from transmitter site. The measuring lines were set parallel with the current dipole, and the horizontal magnetic coil was laid under the ground approximately at the center of the eight electrodes layout. The orientation of the coil was always perpendicular to the direction of the current dipole.

Considering cultural noise conditions, burying the coil, avoiding setting the coil near power lines, checking for electrical loss at the connecting parts and stacking processing of data were carried out during the survey.

However, in the survey area, a national road runs almost through the center of the area from east to west, and several power lines are distributed parallel to the road.

Therefore, most of data was affected by those facilities and some of the data seemed to be terrible. These data were used after correcting, but some of them were eliminated.

(2) Analysis procedure

The analysis of CSAMT data was carried out according to the flow of analysis shown in Fig. II.3.15. The calculation of the near-field correction was carried out using the program which was donated to Turkey from JICA as the program for CSAMT measurement. The 1-D inversion was repeated until the observed data agreed with the theoretical data which was calculated from a model of resistivity structure for each station.

3. Results and interpretation

(1) Apparent resistivity distribution

1) Apparent resistivity map (f = 128 Hz) (Fig. II.3.16)

The measured apparent resistivities range from 1.0 to 14 ohm-m. This map shows the resistivity distribution near the surface down to around 100 m deep.

The low resistivity zone showing less than 4 ohm-m extends roughly east to west, and the extremely low resistivity zone of less than 2 ohm-m is recognized at the center and in the southeastern part.

Most of the geothermal manifestations such as hot springs and fumaroles are located within this low resistivity zone. Therefore, this low resistivity zone is estimated to be closely related to the geothermal activity and hydrothermal alteration zone of the area.

Besides, the southwestern part from Kaynarca, it can be seen the low resistivity zone of less than 3 ohm-m extends northeast to southwest. It seems to indicate the existence of a fault-like structure trending in that direction. The relatively high resistivity zone (more than 8 ohm-m) is recognized along the mountains in north and south. Hence, the high resistivity zones may reflect the volcanic rocks near the surface in the survey area.

2) Apparent resistivity map (f = 4 Hz) (Fig. II.3.17)

The extremely low resistivity zone of less than 2 ohm-m is recognized from Kaynarca to the southeast. By connecting this low

zone to the zone in the northwestern part of less than 7 ohm-m, a fault-like structure can be estimated. Furthermore, another fault-like structure trending east to west can be recognized from the point G 100 to the point K 3,400.

The fault-like structure trending northeast to southwest is not remarkable compared with the previous map (Fig. II.3.16).

The linear structure recognized from contour shape, elongation and distortion may be related to the geothermal structure and may be caused by some fault structures.

3) Apparent resistivity map (f = 0.25 Hz) (Fig. II.3.18)

The apparent resistivities of frequencies around 0.25 Hz are considered to reflect deep (500--1,000 m) structures. The pattern is almost the same as the previous map, but in this map it is easier to see the linear structure that is interpreted as a fault-like structure.

The linear structure trending northwest to southeast is very clear on this map, and probably reflects the fault structure. Especially, the relatively low resistivity zone less than 22 ohm-m in the northwestern part showing the belt zone indicates a fault structure.

The linear structure trending east to west and northwest to southwest are not so clear compared with the map of 4 Hz.

4) Pseudosections

Traverse lines from A to U were set in the direction of east to west parallel with the current dipole. By referring these pseudosections, the resistivity change along east to west direction can be seen clearly.

(a) A line (Fig. II.3.19)

Low apparent resistivities are recognized at points 1,700, 1,900 and 100. The resistivities of east part are generally high compared with the resistivities of west part.

(b) B line (Fig. II.3.20)

Low resistivities can be recognized at points 1,150 and 1,250. These low zones are obtained at frequencies from 4 to 64 Hz, so that these may show anomalies at the shallow resistivity distribution.

(c) C line (Fig. II.3.21)

The resistivity values are mostly around 10 ohm-m.

(d) D line (Fig. II.3.22)

Low resistivities can be recognized at points 150 and 250, and other stations show high resistivities around 10 ohm-m.

(e) E line (Fig. II.3.23)

A low anomaly is recognized at point 2,600. Other anomalies can be recognized but they are small.

(f) F line (Fig. II.3.24)

All points show the resistivities around 10 ohm-m on average except the low frequency bands. At points 450, 750 and 1,150, small low resistivity zones can be seen.

(g) G line (Fig. II.3.25)

Low resistivities are recognized in the east part (points 1,900 to 2,800). The frequencies of those low resistivities range from 18 to 512 Hz, so that the depth of low resistivity zones may be very shallow.

(h) H line (Fig. II.3.26)

Low resistivities are recognized around the points 450 and 1,250. This line is located at the northern edge of the Kaynarca geothermal area.

(i) I line (Fig. II.3.27)

Resistivities are generally low compared with previous lines. Especially from points 1,500 to 2,600, the very low resistivities less than 3.2 ohm-m can be recognized and may be related to the geothermal activity of Kaynarca.

(j) J line (Fig. II.3.28)

This line is located at almost the center of Kaynarca, so that resistivities are quite low in the whole line. Especially, the zone from points 350 to 1,350 shows quite low resistivities less than 3.2 ohm-m. Furthermore, the zone from points 1,000 to 1,150 shows resistivities less than 1.8 ohm-m. These extremely low resistivities must be closely related to the geothermal reservoir structure in the area.

(k) K line (Fig. II.3.29)

This line is also located at almost the center of Kaynarca. Along the line excluding points 300, 500 and 700, very low resistivities less than 3.2 ohm-m can be recognized (1,200 to 2,800). The zone from points 1,600 to 2,400 shows extremely low resistivities less than 1.8 ohm-m, and is thought to reflect the geothermal structure at Kaynarca.

(l) L line (Fig. II.3.30)

All stations show resistivities of less than 3.2 ohm-m, and especially the zone from points 650 to 950 and in the east from point 1,250 it shows resistivities less than 1.8 ohm-m. These resistivities are obtained in the frequency range from 2 to 18 Hz whose frequencies are relatively low compared with previous lines. This shows that the resistivities of low resistivity zone are getting lower and the depths of low resistivity zone are getting deeper in accordance with going from north to south and from west to east.

(m) M line (Fig. II.3.31)

Except the shallow part, this line shows resistivities around 3.2 ohm-m from the center to the east. The zone from the points

from 2,000 to 3,000 gives low resistivities less than 1.8 ohm-m, and is thought to indicate the existence of deep geothermal reservoir.

(n) N line (Fig. II.3.32)

From the center to the east, very low resistivities less than 3.2 ohm-m can be recognized, and the point 1,250 may be the center of the low resistivity zone. The low resistivity zone spreads vertically not horizontally, so that this geothermal area is considered to be dominated by structures such as fractures and faults.

(o) O line (Fig. II.3.33)

The resistivity distribution is almost the same as in the M and N line.

(p) P line (Fig. II.3.34)

The resistivity shows the lowest value at point 950. This can be correlated to the low resistivity zone recognized in the line O.

(q) Q line (Fig. II.3.35)

Resistivity values are getting higher compared with previous lines from J to P. The resistivities of the shallow part are low, but the resistivities of the deep part are high. In the zone from the center to the east, low resistivities can be seen with frequencies from 4 to 32 Hz.

(r) R line (Fig. II.3.36)

Point 650 shows low resistivities near the surface and points 1,050 and 1,150 show also low resistivities with frequencies from 2 to 64 Hz.

(s) S line (Fig. II.3.37)

As a whole, resistivities are relatively high. The zone from the center to point 2,300 shows low resistivities near the surface.

(t) T line (Fig. II.3.38)

Points 750 and 850 show low resistivities near the surface.

(u) U line (Fig. II.3.39)

From the center to the east, the resistivities are relatively high compared with the western part, but those are only near the surface not at depth.

(2) 1-D inversion results

1) Resistivity layers (Fig. II.3.19 to Fig. II.3.39)

The features from 1-D inversion results are explained using several maps. The following sections are characteristic ones to understand the geoelectrical structure in the survey area.

(a) C line (Fig. II.3.21)

This line is located in the northern part of the survey area, and the electrical basement is generally shallow in the west and deep in the east. The resistivity values of the low resistivity zone are relatively high compared with those of the K line described below, and also relatively high compared with those in other geothermal fields. Therefore, south of this line is thought that there is no remarkable geothermal activity and no hydrothermal alteration zones.

(b) K line (Fig. II.3.29)

This line crosses at almost the center of the Kaynarca geothermal area. The remarkable feature in the resistivity distribution is that the zone from points 1,600 to 2,000 almost at the center of Kaynarca shows extremely low resistivities such as 1 to 2 ohm-m. Furthermore, the electrical basement shows an apparent uplift structure which is a typical geoelectrical structure in the geothermal area. This indicates that beneath this line may have a high potential of geothermal resource. The low resistivity potential of geothermal resource. The low resistivity zone may reflect a shallow hot water reservoir or hydrothermally altered zone.

(c) S line (Fig. II.3.37)

This line is located in the southern part of the survey area, and the electrical basement is generally deep in the west and shallow in the east. This tendency is different from the previous two lines. The low resistivity zone shows minimum values at points 2,400 to 2,800 in the east side of the line. Considering resistivity structures from this line and the K line, a remarkable geothermal structure is considered to extend from northwest to southeast.

2) Longitudinal conductance map (Fig. II.3.40)

The sounding curves measured in the area show mostly four layers such as high-low-low-high or low-high-low-high. The sounding curves of these structures are different from the curves measured in other geothermal fields where those sounding curves show generally high-low-high. From this, the resistivities and thickness are used for the evaluation as a value of longitudinal conductance.

As shown in the figure, a high conductance zone (130 ohm) can be recognized at the Kaynarca and the south. And it elongates from northwest to southeast. This high conductance zone is located in between the fault-like structures trending northwest to southeast and northeast to southwest which are interpreted from apparent resistivity maps.

Thus, the extent and elongation of the high conductance zone is estimated to be formed by two faults which are important from a geothermal point of view.

3) Electrical basement (Fig. II.3.41)

The electrical basement is defined as the deepest layer with relatively high resistivity values, and is usually not correlated with the geological basement. In general, the geothermal reservoir is formed in the electrical basement and sometimes electrical discontinuity is correlated to the productive geothermal reservoir. In this meaning, the study on the discontinuity of the electrical basement is usually important in developing the geothermal resource. In the central part of the survey area, from Kaynarca to the southeast an electrical uplift structure is observed.

On the contrary, in the northern part and southwestern part the electrical basement is recognized as electrical depression zone. The electrical uplift zone was detected as a depression zone from the gravity survey and the geological study. Geoelectrically, if a geothermal structure is not formed in the area, the electrical basement may be possibly detected as a depression zone. However, if a geothermal structure is formed in the survey area, the promising zone is usually detected as an apparent uplift structure. The reasons are described below.

(a) Because of low resistivity zones, the low resistivities layers are calculated as thin layers, and the high resistivity layers as thick by the reason of the principle of equivalence.

(b) When a geothermal reservoir is formed even in the depression zone, its structure is detected as an apparent uplift structure by the reason described above. It doesn't reflect an actual depression structure.

Therefore, careful interpretation of apparent uplift structures using resistivity data for geothermal exploration is required.

This uplift structure indicates the existence of a geothermal structure such as an altered zone, fault, hot springs and so forth. The key point is its interpretation on the continuity and elongation of electrical anomaly zones.

In this meaning, the uplift extends from Kaynarca to the southeast is correlated to the fault-like structure estimated from the apparent resistivity maps. Another direction of northeast to southwest is not remarkable from this map.

Compared with the electrical basement structure in other geothermal areas, this area shows weak electrical discontinuity. Hence, the difficulty of development of geothermal energy is slightly presumed.

4) Resistivity map of electrical basement (Fig. II.3.42)

A resistivity map of the electrical basement is prepared for the general interpretation of the geological structure, thermal con-

dition and fluid flow at depth. However, the resistivities obtained from the 1-D inversion are actually not accurate compared with those of low resistivity zones, and sometimes number of figures changes from one or two decades in logarithmic scale. Therefore, when the interpretation is carried out using resistivities of the electrical basement, a rough interpretation must be carried out.

Low resistivity zones can be recognized at Kaynarca, the western part, southwestern part and northern part. In these area rock resistivities in deeper part are estimated to be still low, and some of them may be related to the geothermal structure of the area. Especially, when some linear structures can be recognized from the resistivity contour, it is quite possible that those low resistivity zones reflect the fractured reservoir at depth.

In this meaning, around Kaynarca, the low resistivities are recognized to extend in a northwest to southeast direction. This structure can be seen in the map as shown in Fig. II.3.43.

Other low resistivities can be recognized in the west and northwest from Kaynarca. In the shallow parts of these area, low resistivities can not be recognized and in deeper parts low resistivities may exist. This suggests that the western and southwestern part of Kaynarca is promising for geothermal development.

(3) 2-D modeling analysis

The pattern of resistivity distribution in the M line which is located almost at the center of Kaynarca, is considered to represent the typical resistivity distribution of the geothermal structure in the area. Therefore, a resistivity block model as shown in Fig. II.3.44 was made in order to study the geothermal structure of the area. The 2-D modeling analysis was carried out and the result is shown in Fig. II.3.45. The pseudosection of the upper part shows the measured apparent resistivities and the lower part shows the theoretical apparent resistivities based on the 2-D model. The patterns of resistivity distribution of these two pseudosections are very similar, so that the resistivity structure of the area is estimated to be the structure shown in Fig. II.3.44.

The features of the resistivity model are summarized as follows:

1) The vertical structure of about 1 ohm-m is located at point 2,300.

2) In the eastern part from point 2,300, the electrical basement of about 50 ohm-m shows an uplift structure, on the contrary, in the western part, the thickness of the low resistivity zone ranges from 300 to 400 m.

3) The geothermal structure in the Kaynarca geothermal area is estimated to be characterized by a vertical fault and along this fault the geothermal reservoir may be formed.

(4) Conclusion (Fig. II.3.46)

1) Three major faults are determined from the apparent resistivity maps as follows.

(a) Fault trending E-W near the northern edge of Kaynarca.

(b) Fault trending NW-SE crossing the center of Kaynarca.

(c) Fault trending NE-SW crossing the center of Kaynarca. This fault indication is not remarkable compared with other estimated faults.

2) The southern part between the estimated faults trending northwest to southeast and northeast to southwest is recognized as a high longitudinal conductance zone. This zone is considered to be important, because it is estimated that the extent of the high longitudinal conductance zone is closely related to the extent of shallow hot water reservoir and hydrothermal alteration zone.

3) From the resistivities at depth, the fault trending northwest to southeast can be estimated. And, a structure which extends from Kaynarca to the west or southwest is thought to exist. However, this indication is relatively weak compared with others.

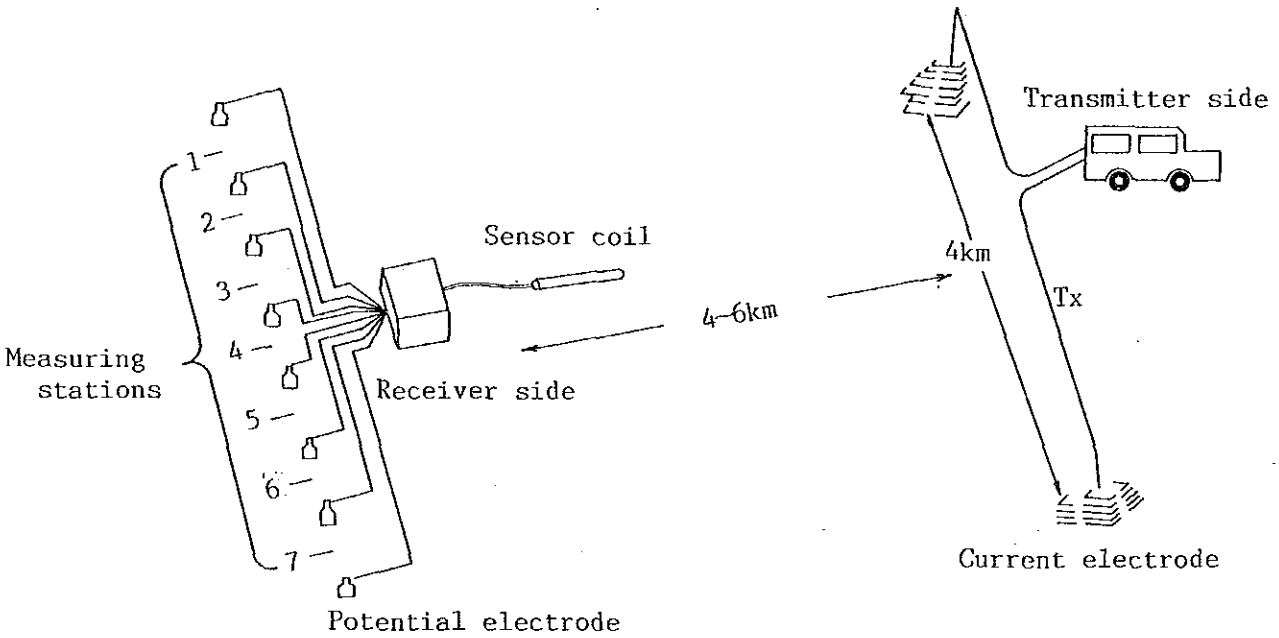

Fig.Ⅱ.3.14 Survey configuration for CSAMT measurement

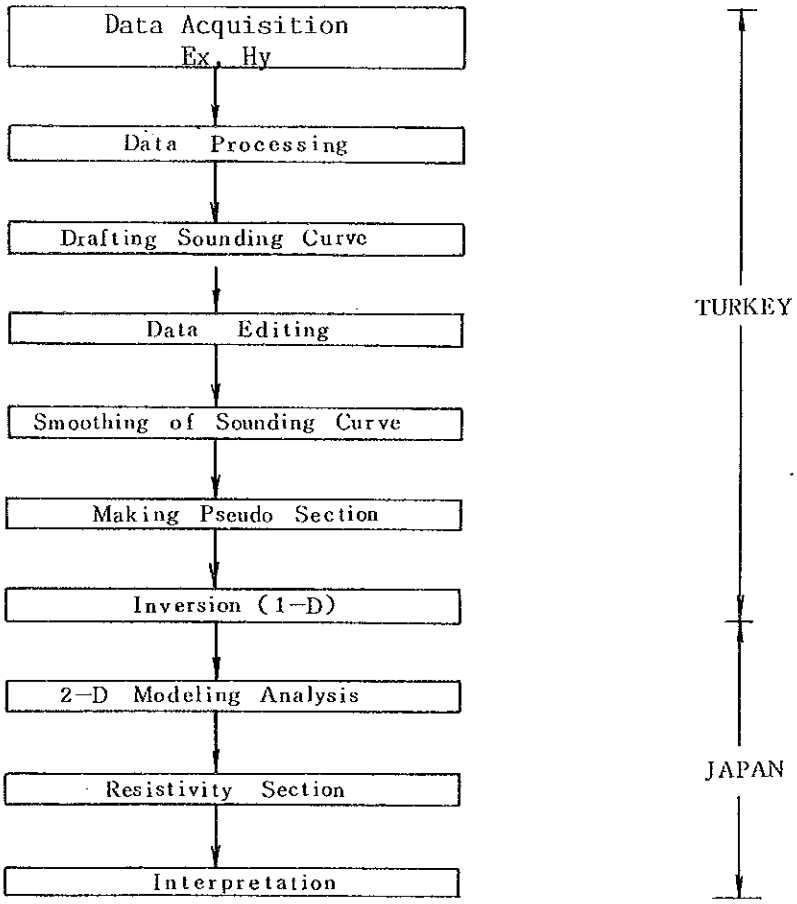

Fig.Ⅱ.3.15 Flow of analysis for CSAMT measurement

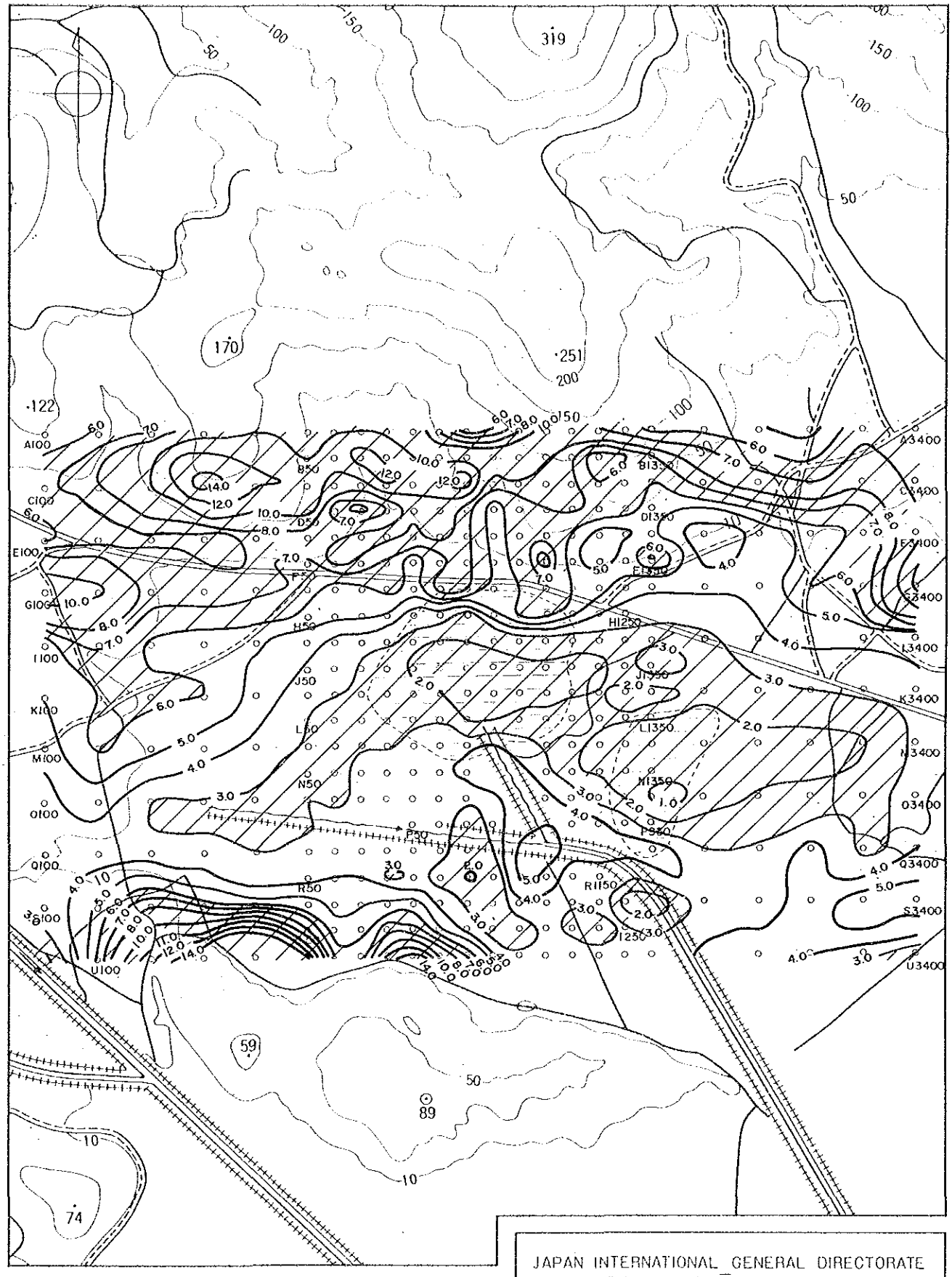

Legend

A100 / O station number and location

~3~ Contour line of apparent resistivity (Unit:ohm-m)

JAPAN INTERNATIONAL COOPERATION AGENCY

GENERAL DIRECTORATE OF MINERAL RESEARCH AND EXPLORATION

GEOTHERMAL DEVELOPMENT PROJECT IN DIKILI-BERGAMA FIELD

0 500 1000m

Fig II .3.16 Apparent resistivity map (128 Hz)

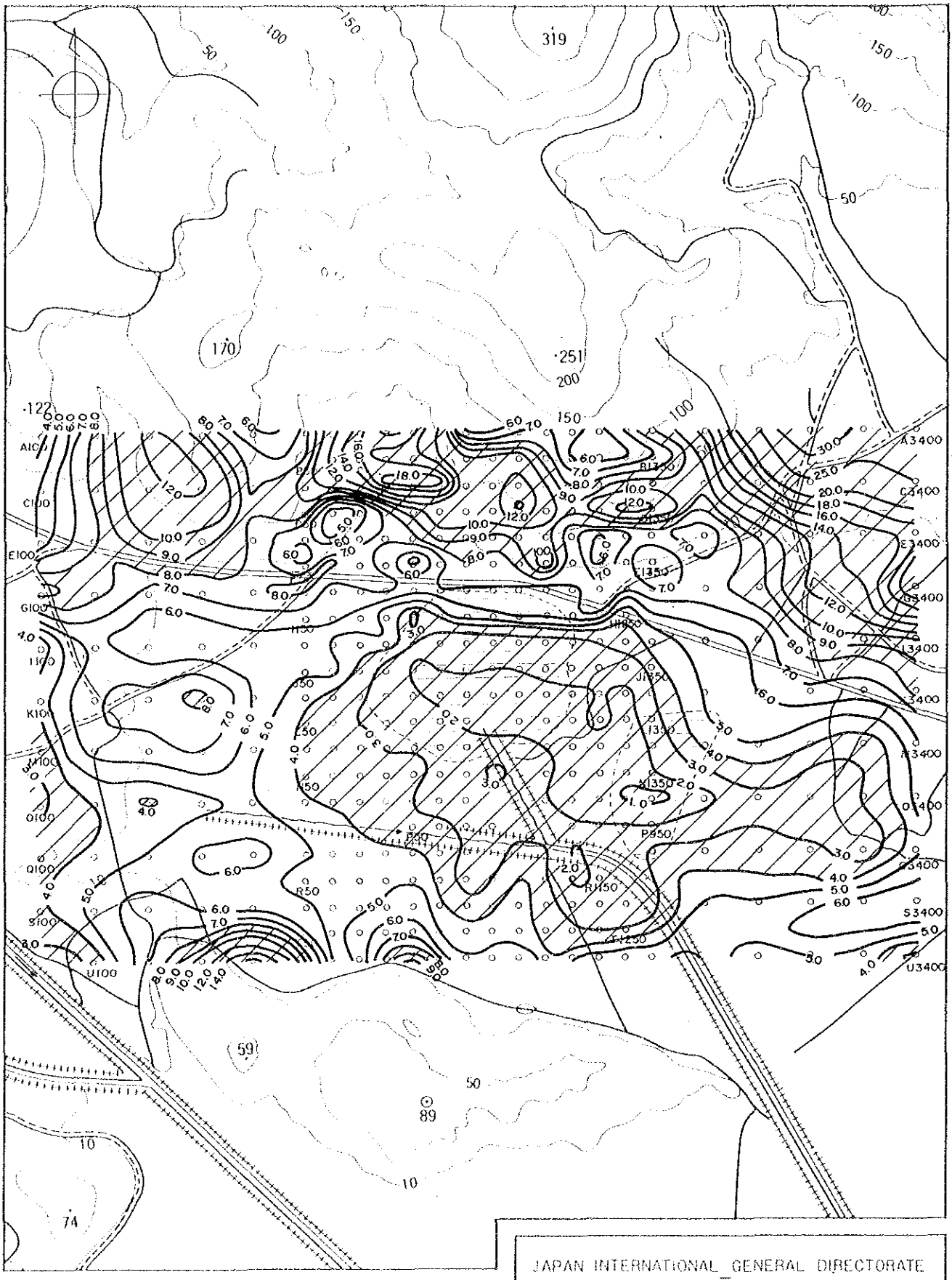

Legend

A100 / O station number and location

~3.0~ Contour line of apparent resistivity (Unit:ohm-m)

JAPAN INTERNATIONAL COOPERATION AGENCY

GENERAL DIRECTORATE OF MINERAL RESEARCH AND EXPLORATION

GEOTHERMAL DEVELOPMENT PROJECT IN DIKILI-BERGAMA FIELD

0 500 1000m

Fig II.3.17 Apparent resistivity map (4Hz)

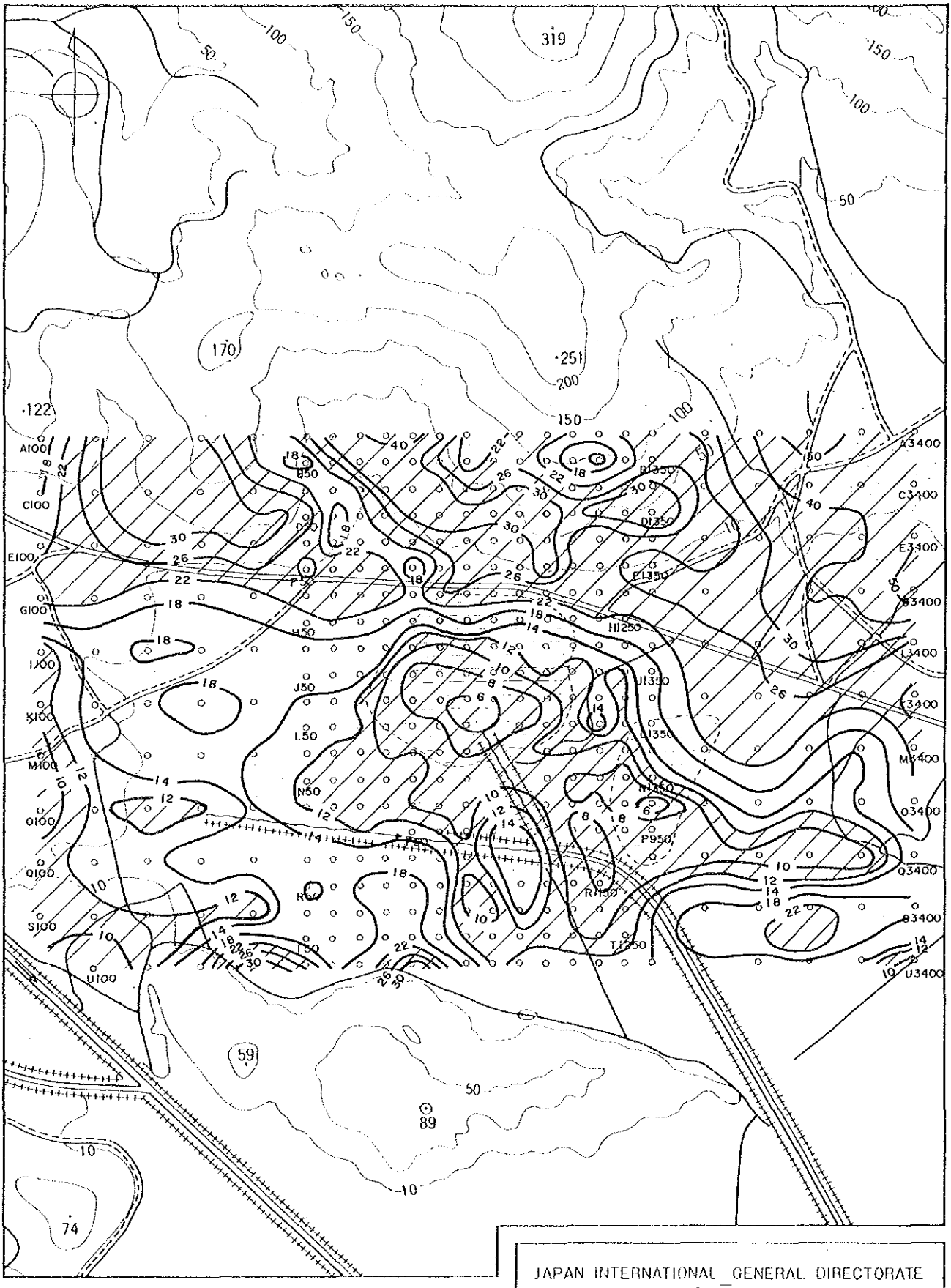

Legend

A100 / O station number and location

~8~ Contour line of apparent resistivity (Unit:ohm-m)

JAPAN INTERNATIONAL COOPERATION AGENCY

GENERAL DIRECTORATE OF MINERAL RESEARCH AND EXPLORATION

GEOTHERMAL DEVELOPMENT PROJECT IN DIKILI-BERGAMA FIELD

0 500 1000m

Fig II .3.18 Apparent resistivity map (0.25Hz)

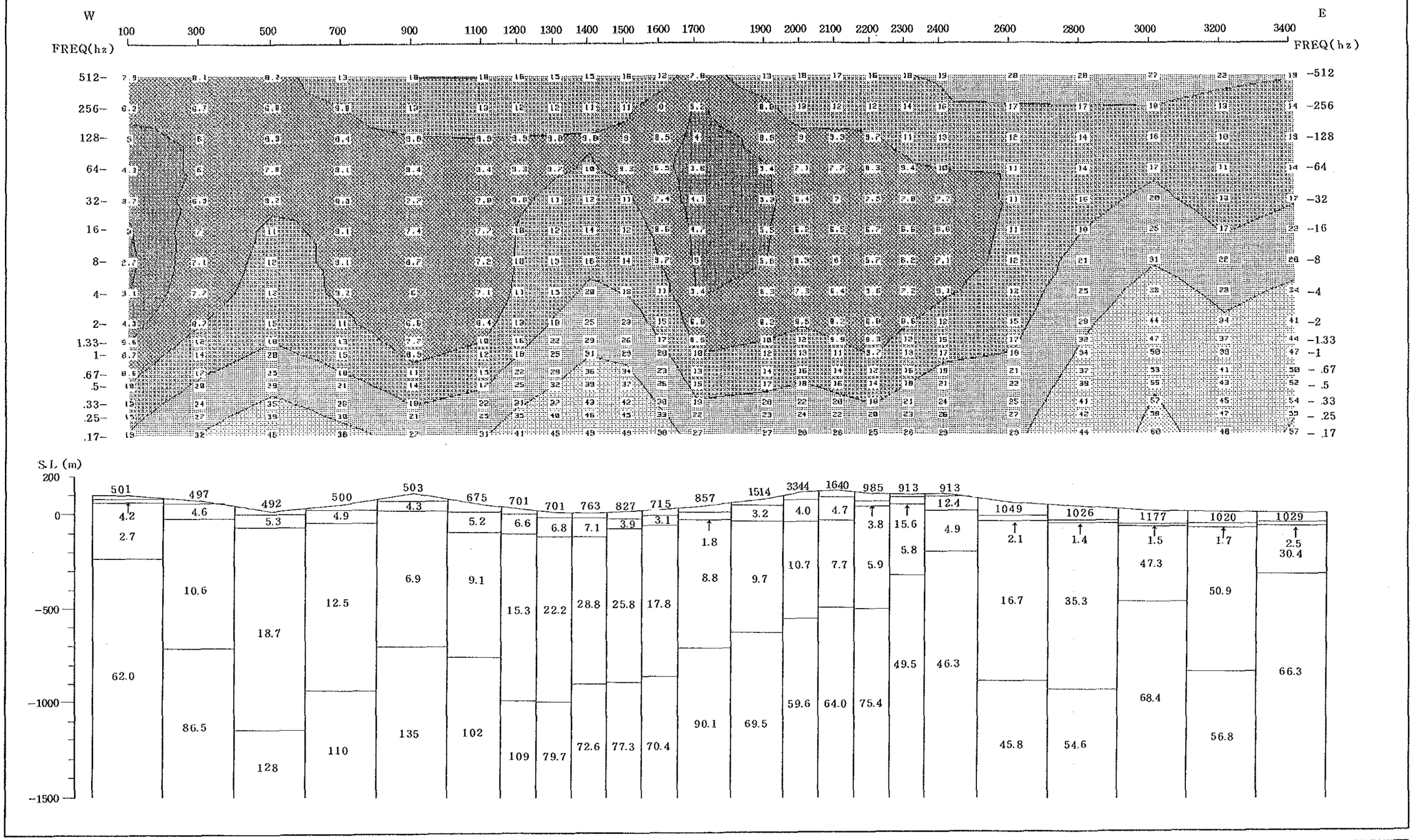

Fig II.3.19 Apparent resistivity pseudosection and 1D inversion results (A line) (Unit:ohm-m)

JAPAN INTERNATIONAL COOPERATION AGENCY
GENERAL DIRECTORATE OF MINERAL RESEARCH AND EXPLORATION

GEOTHERMAL DEVELOPMENT PROJECT
IN
DIKILI-BERGAMA FIELD

0 500 1000m

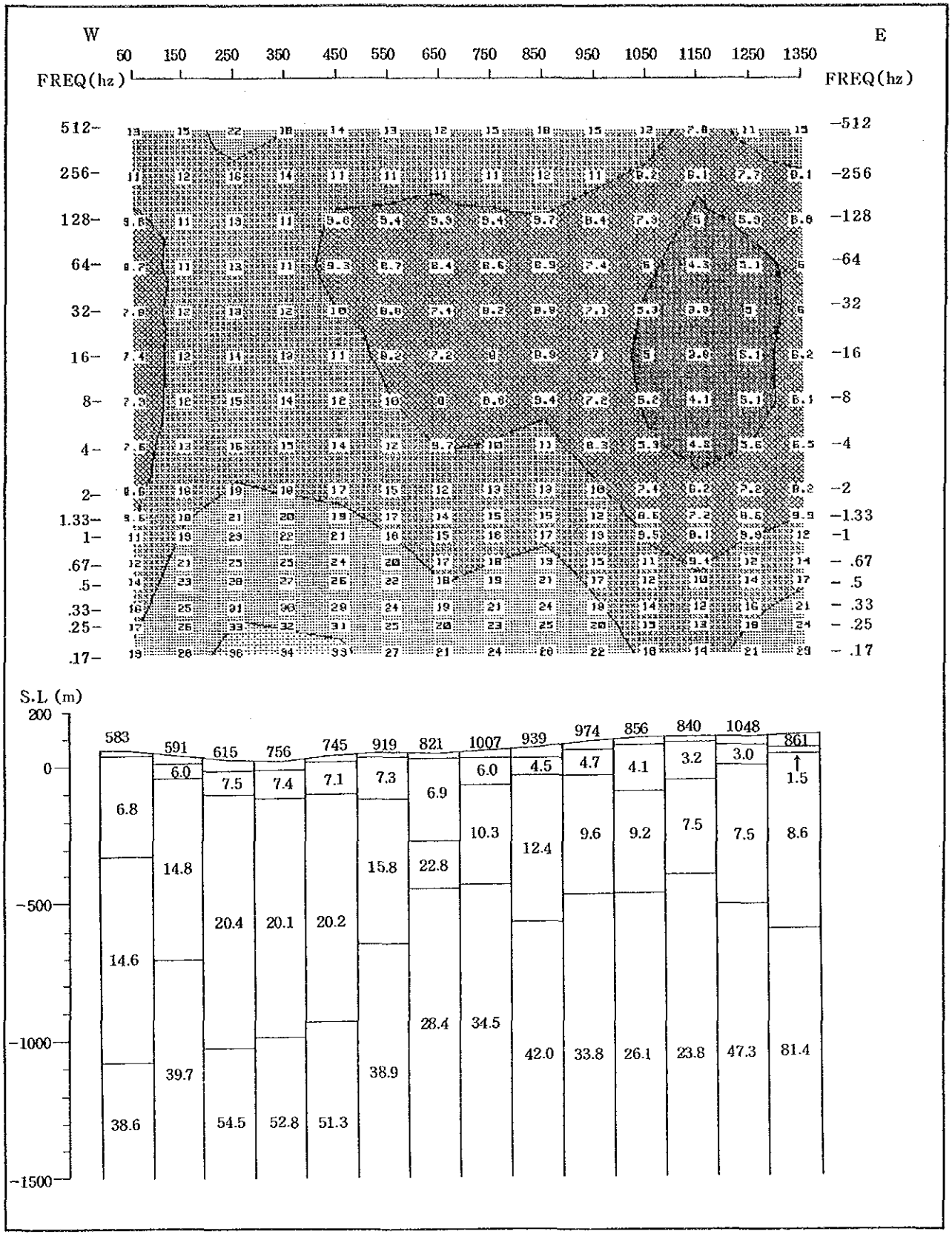

(Unit:ohm-m)

Fig.II.3.20 Apparent resistivity pseudosection and 1D inversion results (B line)

JAPAN INTERNATIONAL COOPERATION AGENCY

GENERAL DIRECTORATE OF MINERAL RESEARCH AND EXPLORATION

GEOTHERMAL DEVELOPMENT PROJECT IN DIKILI-BERGAMA FIELD

0 500 1000m

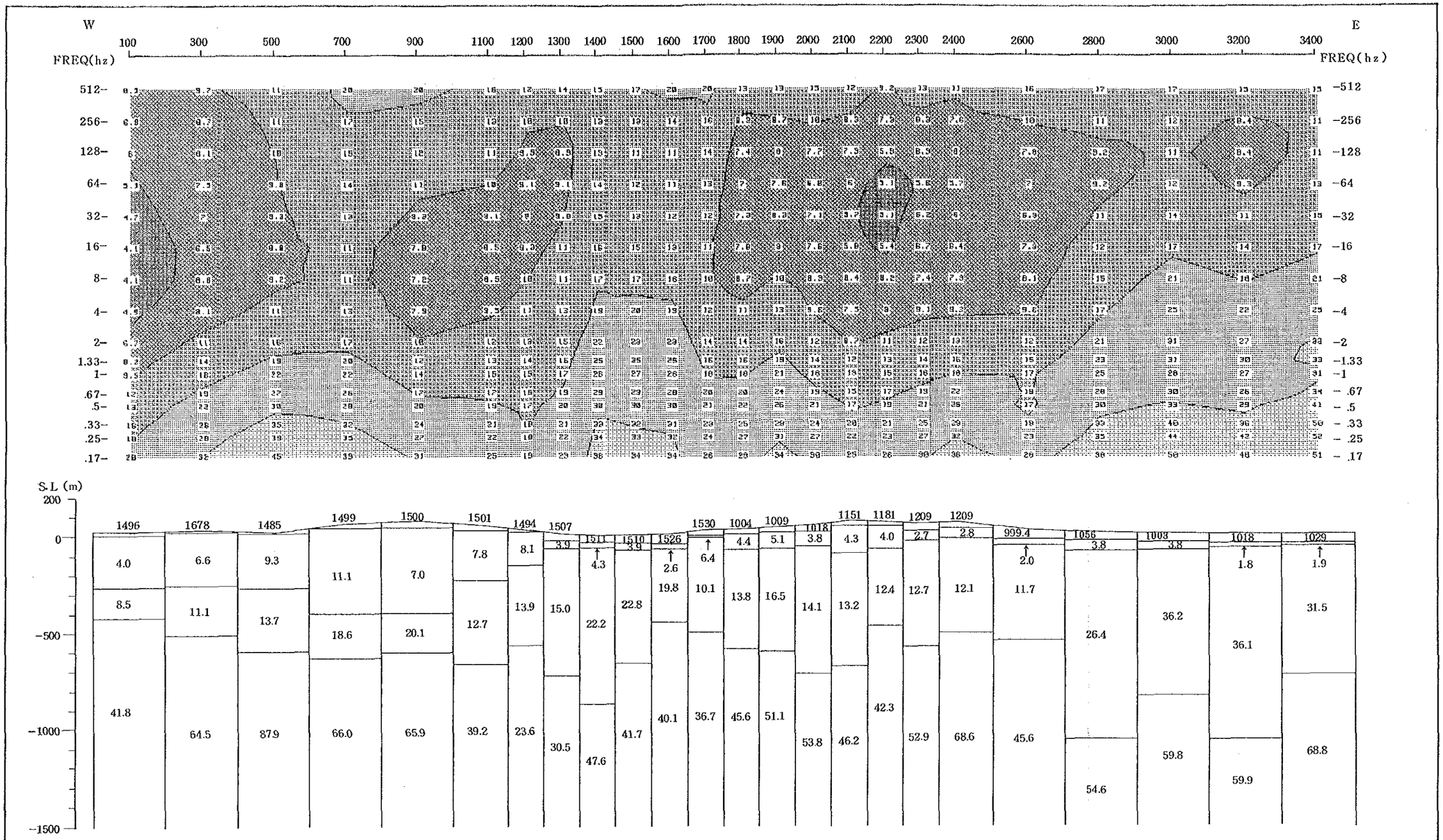

Fig II .3.21 Apparent resistivity pseudosection and 1D inversion results (C line) (Unit:ohm-m)

JAPAN INTERNATIONAL COOPERATION AGENCY

GENERAL DIRECTORATE OF MINERAL RESEARCH AND EXPLORATION

GEOTHERMAL DEVELOPMENT PROJECT IN DIKILI-BERGAMA FIELD

0 500 1000m

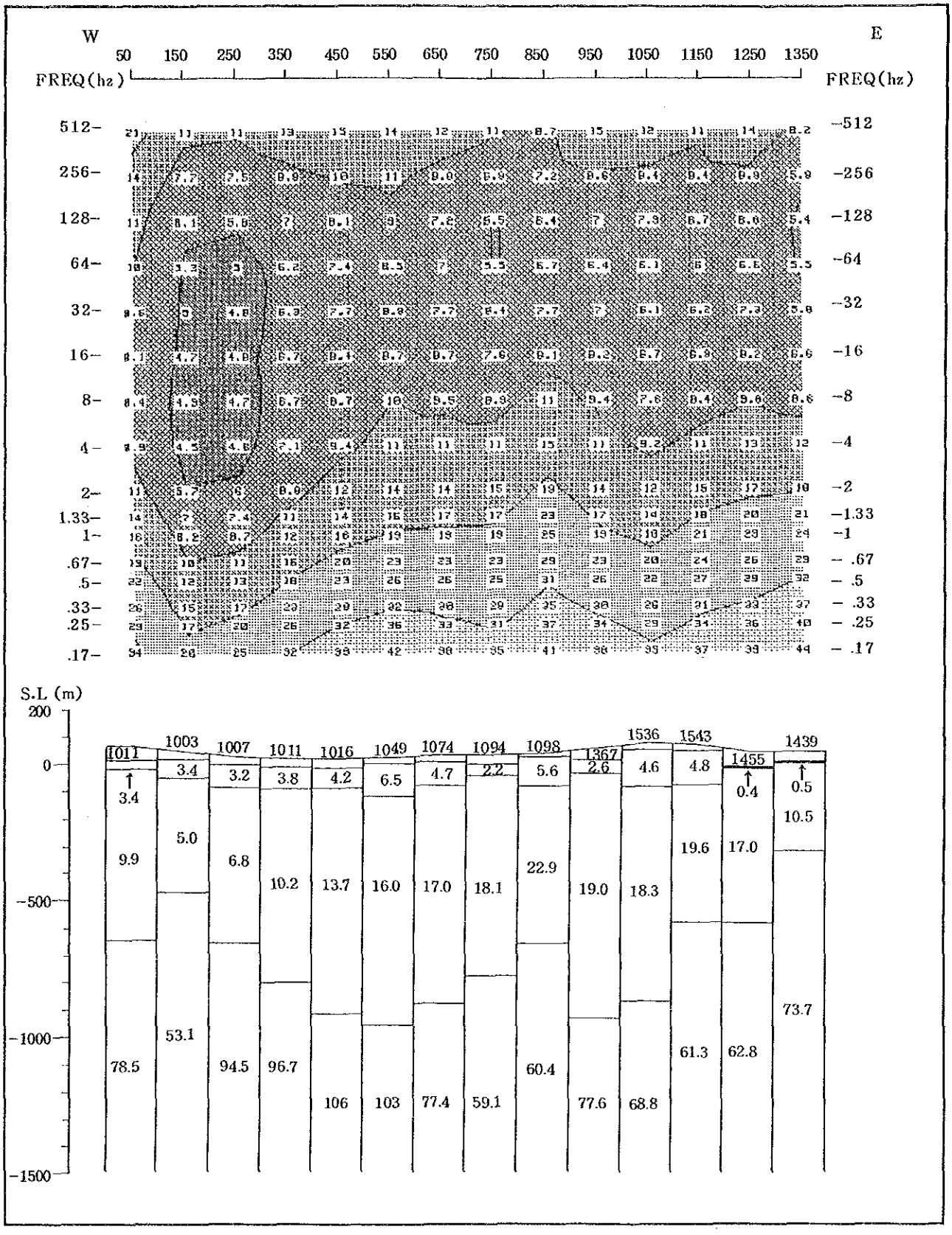

JAPAN INTERNATIONAL COOPERATION AGENCY

GENERAL DIRECTORATE OF MINERAL RESEARCH AND EXPLORATION

GEOTHERMAL DEVELOPMENT PROJECT IN DIKILI-BERGAMA FIELD

0 500 1000m

Fig II.3.22 Apparent resistivity pseudosection and 1D inversion results (D line)
(Unit:ohm-m)

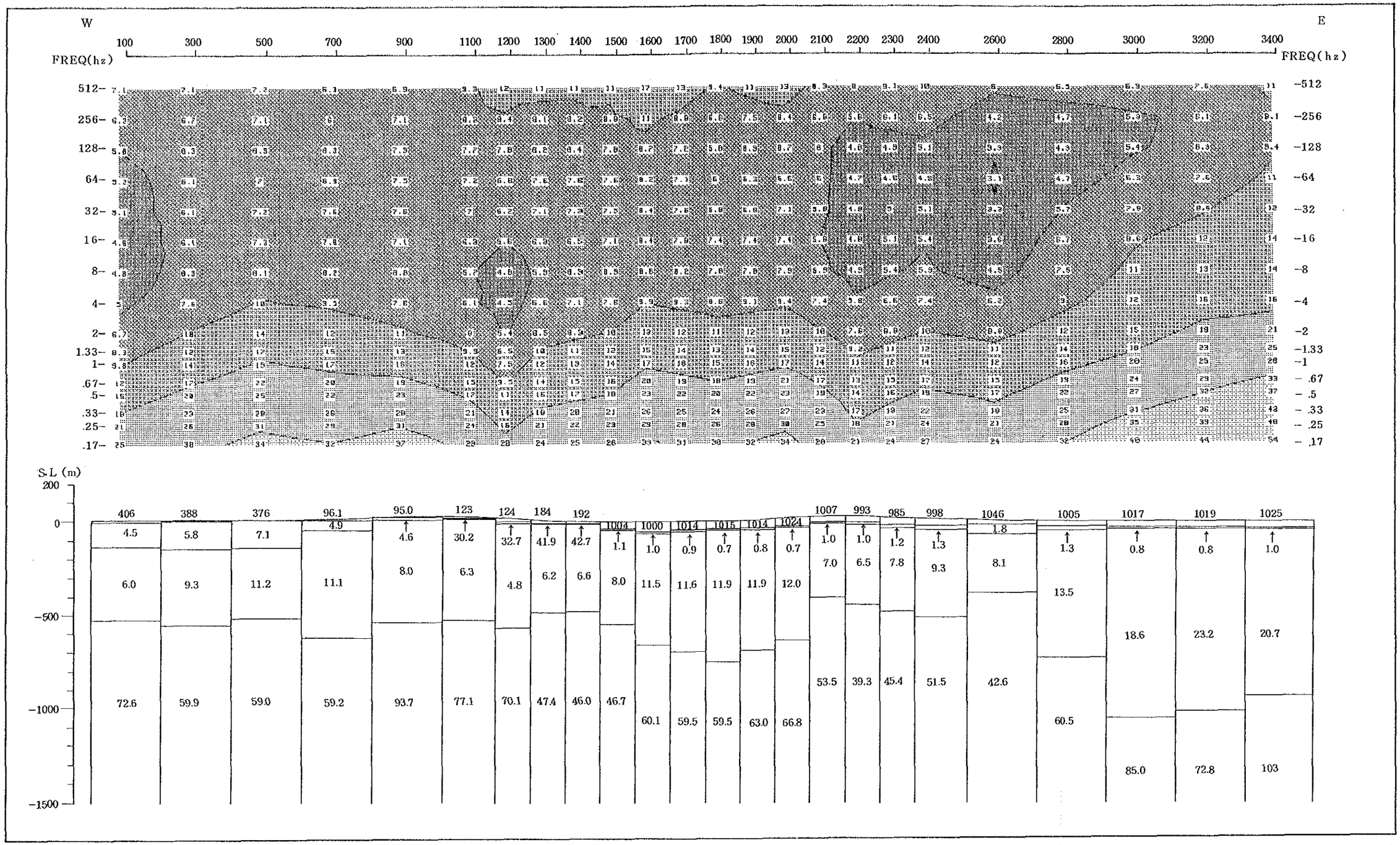

Fig II .3.23 Apparent resistivity pseudosection and 1D inversion results (E line) (Unit:ohm-m)

JAPAN INTERNATIONAL COOPERATION AGENCY
GENERAL DIRECTORATE OF MINERAL RESEARCH AND EXPLORATION

GEOTHERMAL DEVELOPMENT PROJECT
IN
DIKILI-BERGAMA FIELD

0 500 1000m

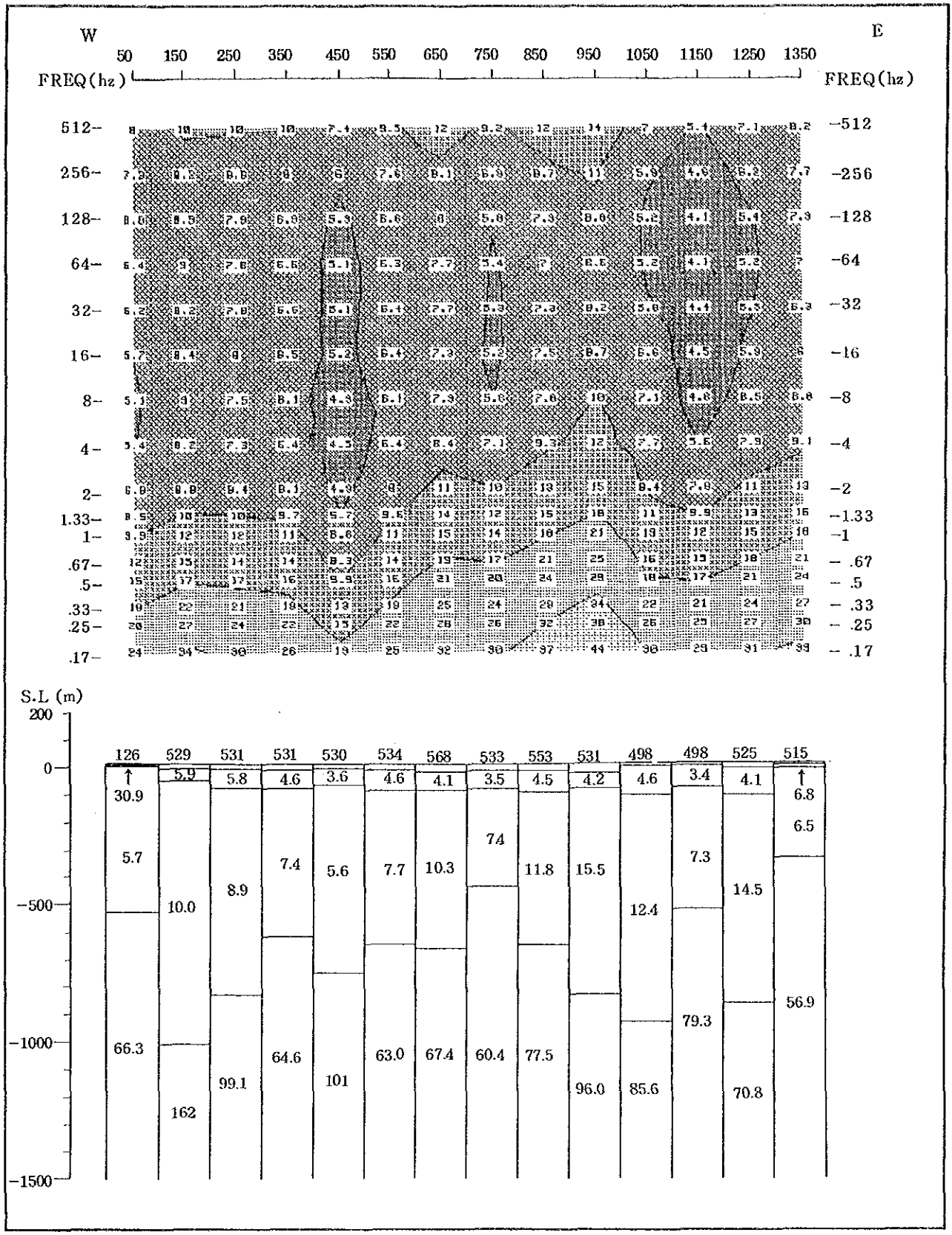

JAPAN INTERNATIONAL COOPERATION AGENCY

GENERAL DIRECTORATE OF MINERAL RESEARCH AND EXPLORATION

GEOTHERMAL DEVELOPMENT PROJECT
IN
DIKILI-BERGAMA FIELD

0 500 1000m

Fig II .3.24 Apparent resistivity pseudosection and 1D inversion results (F line)
(Unit:ohm-m)

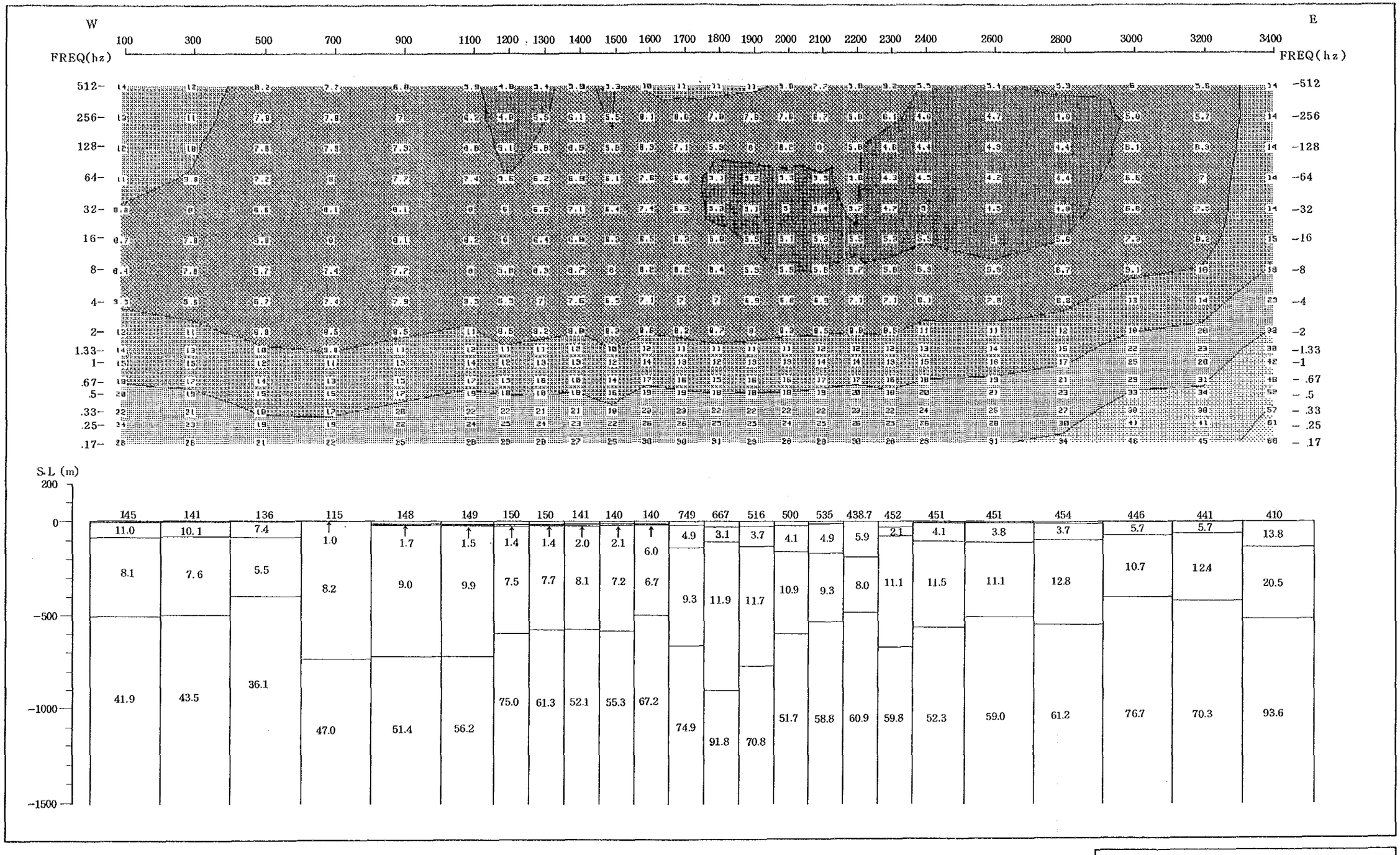

Fig II.3.25 Apparent resistivity pseudosection and 1D inversion results (G line) (Unit:ohm-m)

JAPAN INTERNATIONAL COOPERATION AGENCY

GENERAL DIRECTORATE OF MINERAL RESEARCH AND EXPLORATION

GEOTHERMAL DEVELOPMENT PROJECT IN DIKILI-BERGAMA FIELD

0 500 1000m

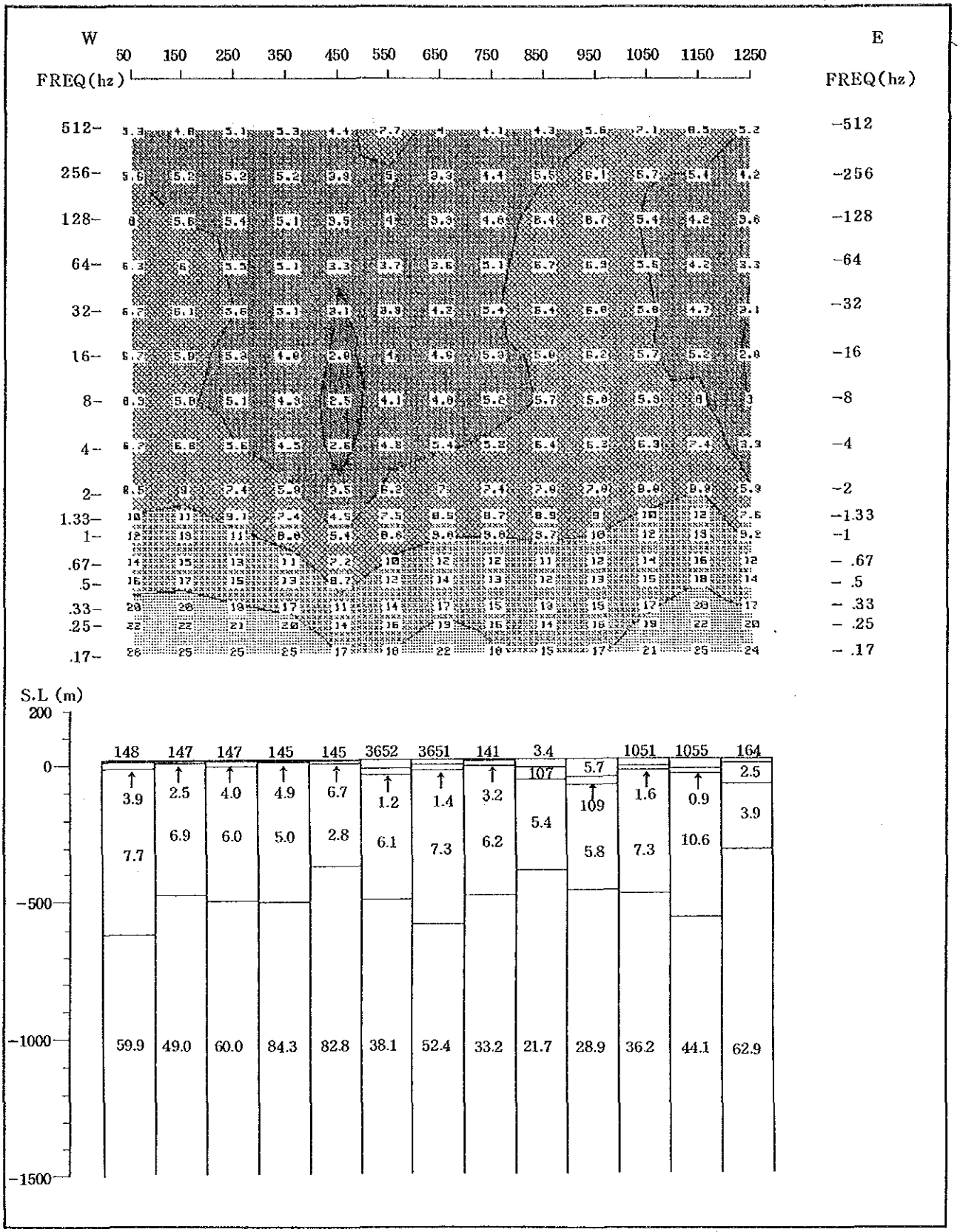

Fig II .3.26 Apparent resistivity pseudosection and 1D inversion results (H line)
(Unit:ohm-m)

JAPAN INTERNATIONAL COOPERATION AGENCY

GENERAL DIRECTORATE OF MINERAL RESEARCH AND EXPLORATION

GEOTHERMAL DEVELOPMENT PROJECT
IN
DIKILI-BERGAMA FIELD

0 500 1000m

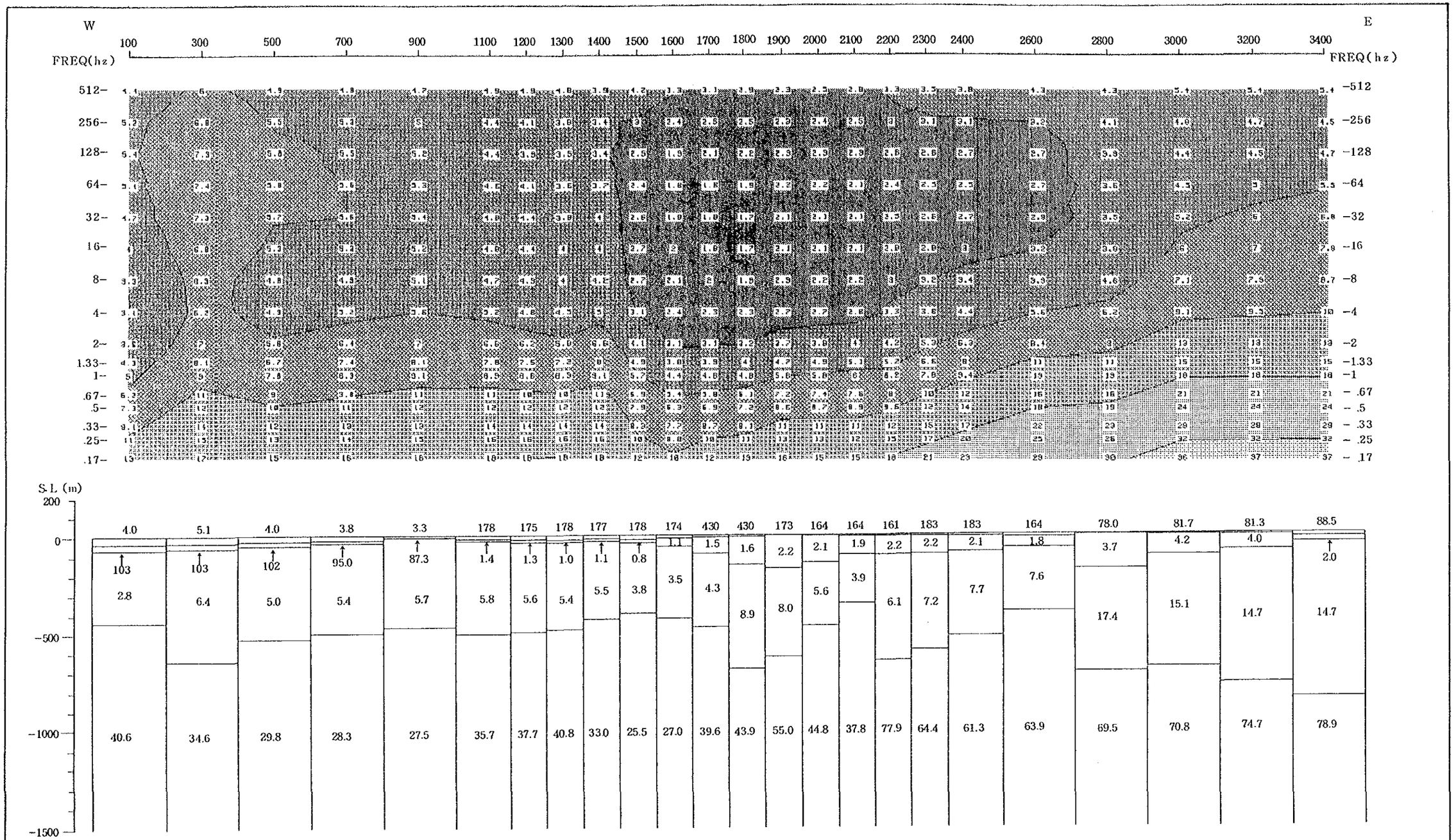

Fig II .3.27 Apparent resistivity pseudosection and 1D inversion results (I line) (Unit:ohm-m)

JAPAN INTERNATIONAL COOPERATION AGENCY
GENERAL DIRECTORATE OF MINERAL RESEARCH AND EXPLORATION

GEOTHERMAL DEVELOPMENT PROJECT
IN
DIKILI-BERGAMA FIELD

0 500 1000m

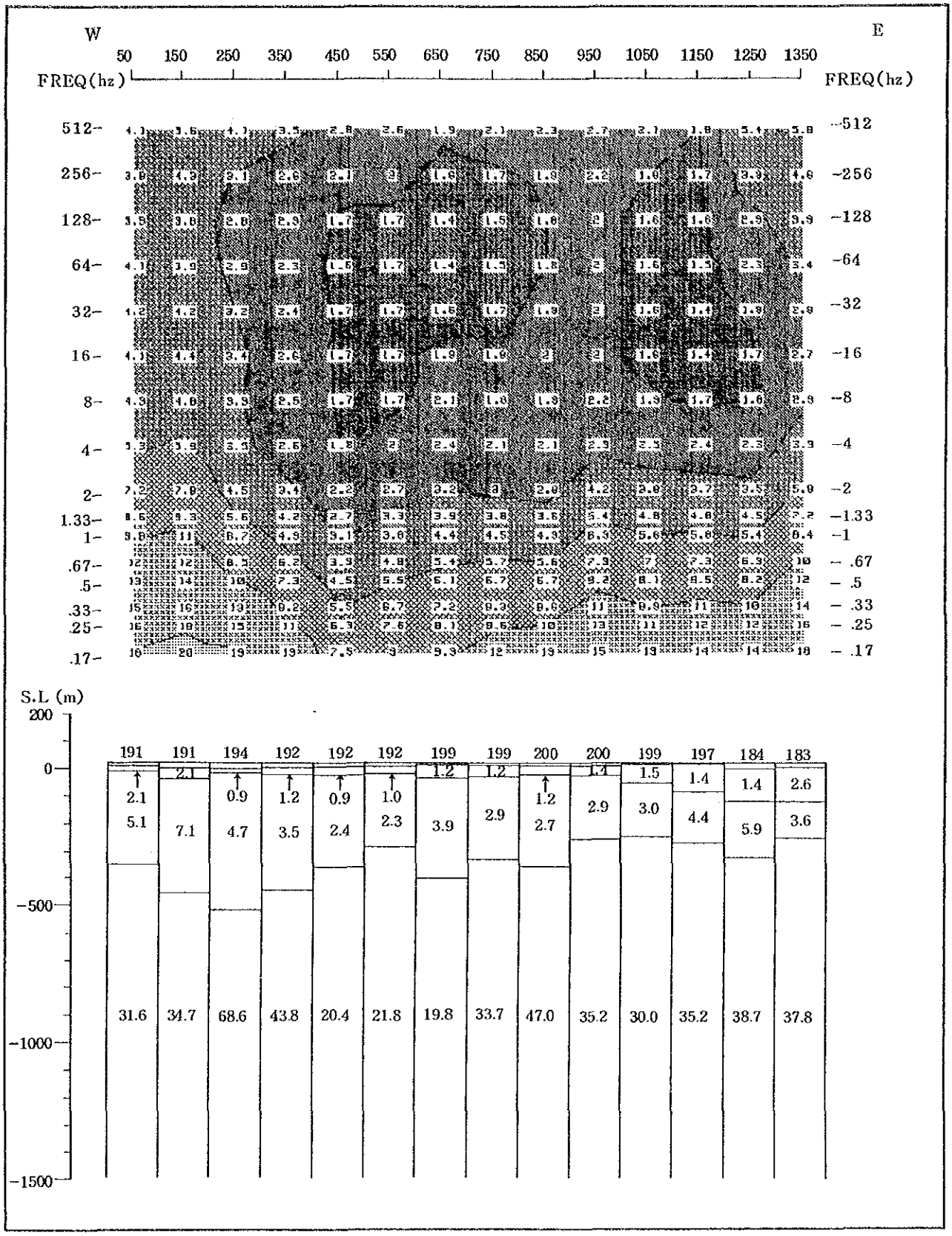

JAPAN INTERNATIONAL COOPERATION AGENCY

GENERAL DIRECTORATE OF MINERAL RESEARCH AND EXPLORATION

GEOTHERMAL DEVELOPMENT PROJECT IN DIKILI-BERGAMA FIELD

0 500 1000m

Fig II .3.28 Apparent resistivity pseudosection and 1D inversion results (J line) (Unit:ohm-m)